Electronic Supplementary Material (ESI) for Journal of Materials Chemistry A.


# Supporting Information

# Pseudocapacitive Porous Hard Carbon Anode with Controllable Pyridinic Nitrogen and Thiophene Sulfur Co-doping for High-power Dual-carbon Sodium Ion Hybrid Capacitors

Chong Wang, [a] Ning Zhao, [a] Bohan Li, [a] Qingtao Yu, [a] Wanci Shen, [a] Feiyu Kang, [a,b] Ruitao Lv, *[a] and Zheng-Hong Huang *[a,b]

[a] State Key Laboratory of New Ceramics and Fine Processing, School of Materials Science and Engineering, Tsinghua University, Beijing 100084, China

[b] Engineering Laboratory for Functionalized Carbon Materials, Shenzhen Key Laboratory for Graphene-based Materials, Graduate School at Shenzhen, Tsinghua University, Shenzhen 518055, China

[c] Key Laboratory of Advanced Materials (MOE), School of Materials Science and Engineering, Tsinghua University, Beijing 100084, China

E-mail: zhhuang@mail.tsinghua.edu.cn

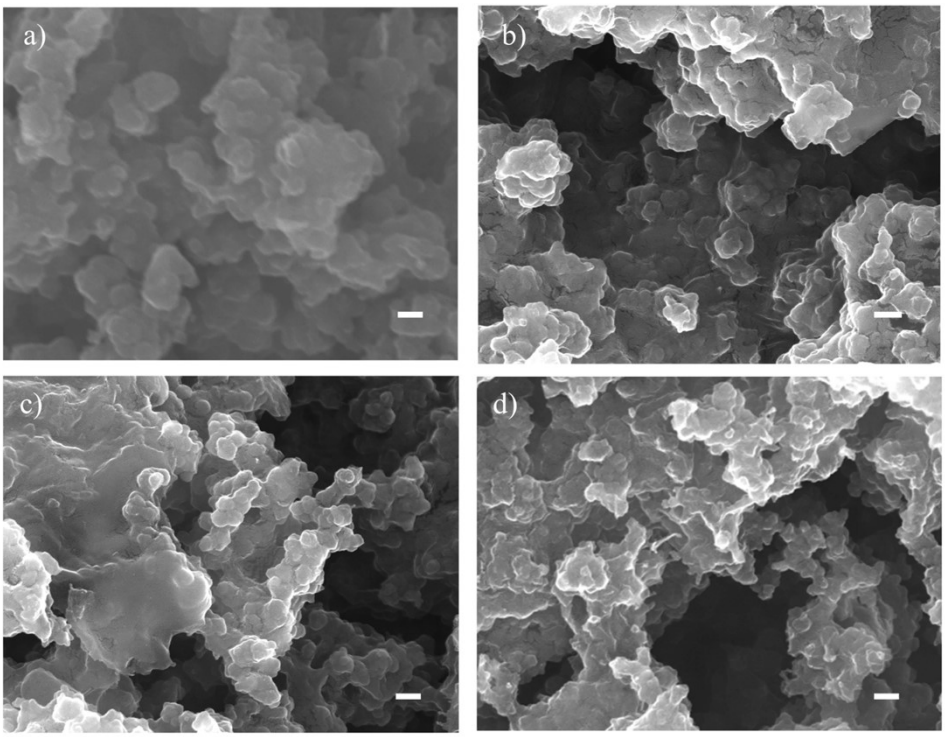


**Fig. S1.** The SEM images of (a) N-HC, (b) NS-pHC-0.337, (c) NS-pHC-0.674, (d) NS-pHC-1.348. The scale bar is 200 nm.

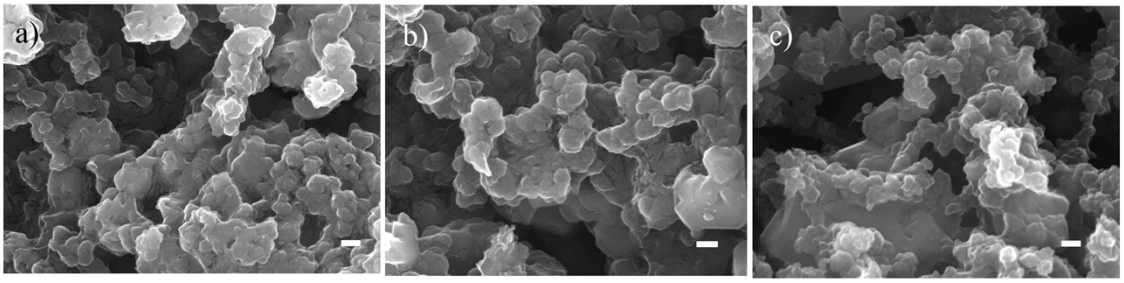


**Fig. S2.** The SEM of (a) NS-pHC-Mg-0.337, (b) NS-pHC-Mg-0.674, (c) NS-pHC-Mg-1.348. The scale bar is 200 nm.

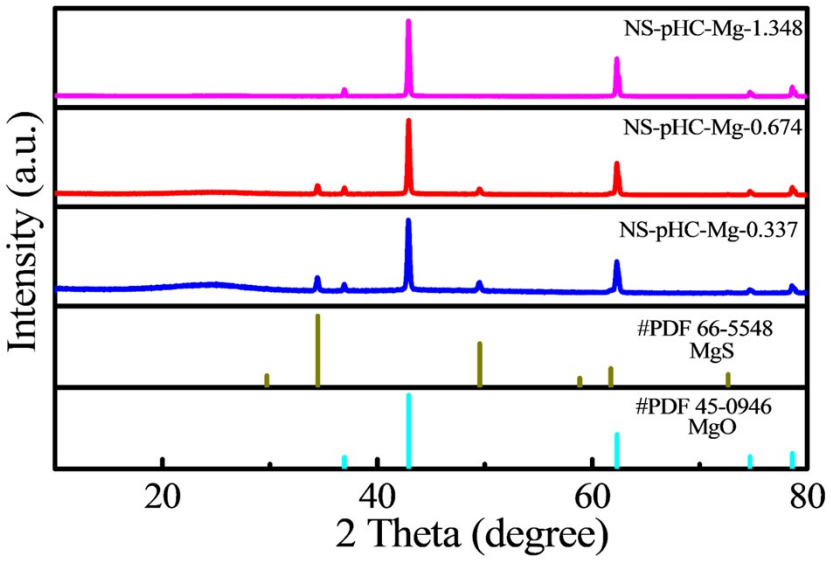


**Fig. S3.** The XRD patterns of NS-pHC-Mg-*x*.

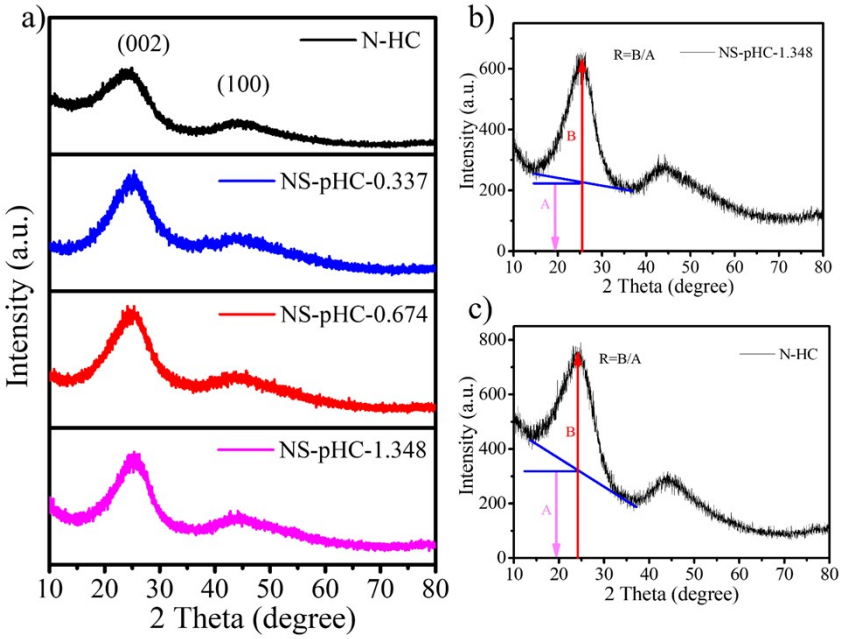


**Fig. S4.** (a) The XRD patterns of N-HC and NS-pHC-x. The calculated manner of R value for (b) NS-pHC-1.348 and (c) N-HC.

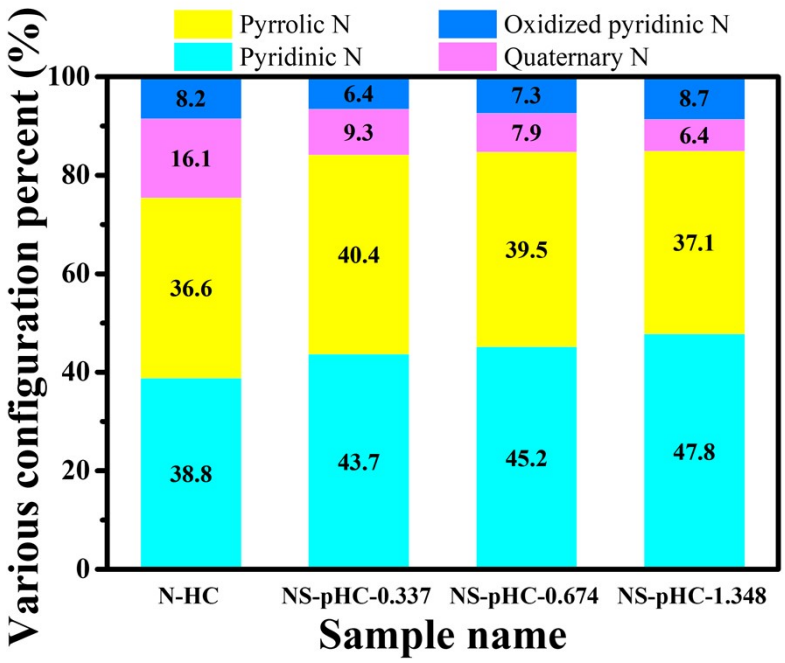


**Fig. S5.** The ratios of various configurations of nitrogen dopants for N-HC and NS-pHC-x.

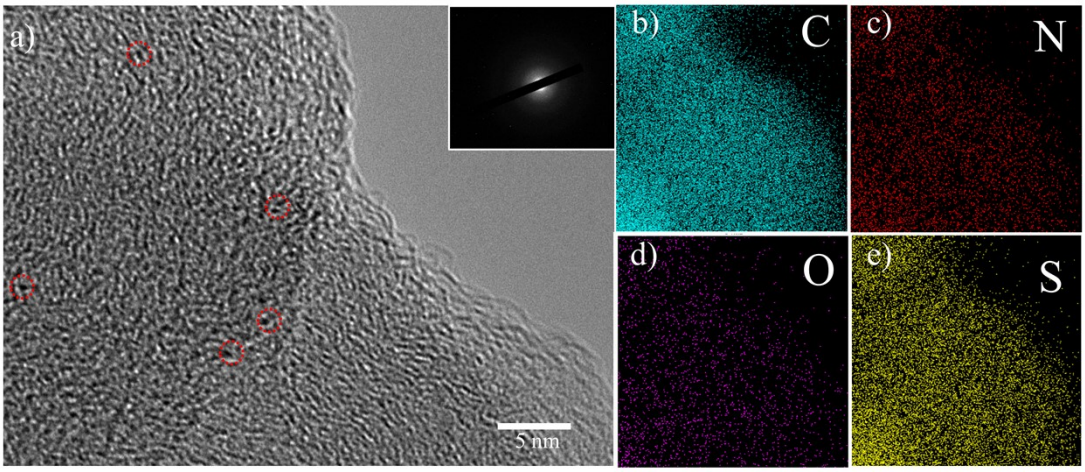


**Fig. S6.** The HRTEM (a) of NS-pHC-1.348. The HRTEM element distribution of (b) carbon, (c) nitrogen, (d) oxygen and (e) sulfur.

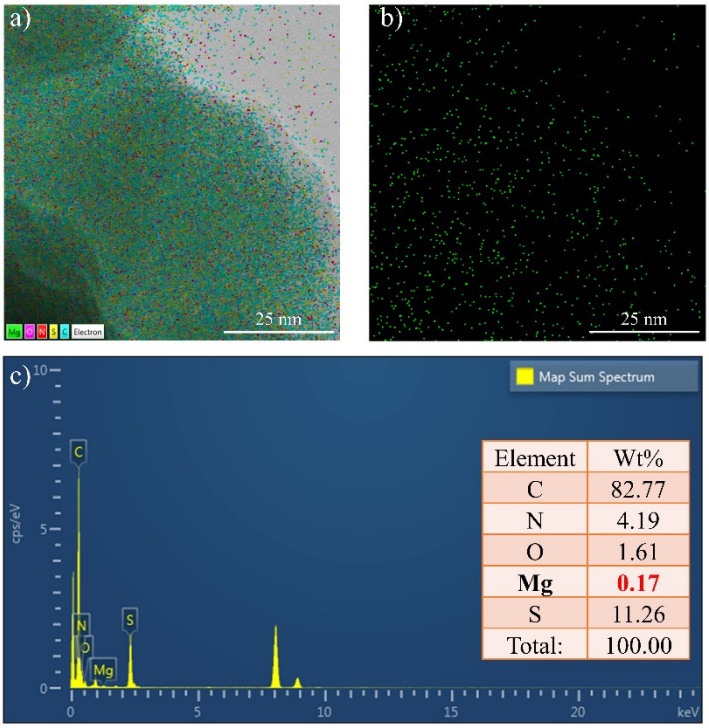


**Fig. S7.** The HRTEM element distribution of (a) total elements and (b) Mg element in NS-pHC-1.348. (c) The map sum spectrum of total elements (The relative ratios of C, N, O were different from that obtained from XPS data because elemental mapping is less sensitive to the light elements with a small weight difference).

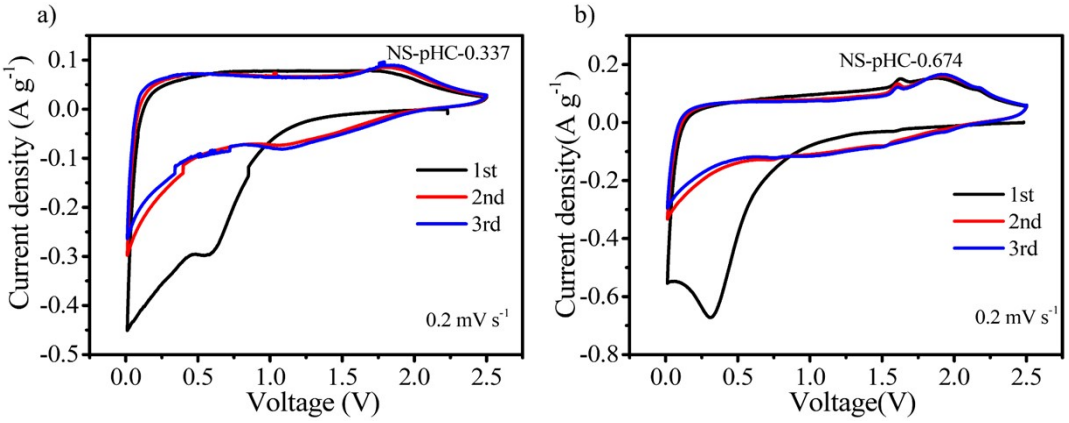


**Fig. S8.** The CV curves of first 3 cycles at 0.2 mV $s^{-1}$. (a) NS-pHC-0.337, (b) NS-pHC-0.674.

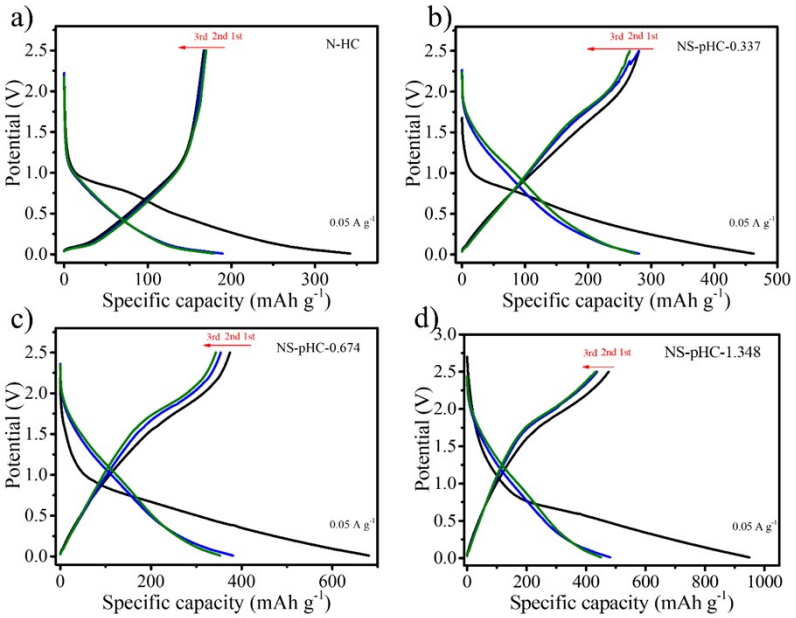


**Fig. S9.** The GCD curves of first 3 cycles at 0.05 A $g^{-1}$. (a) N-HC, (b) NS-pHC-0.337, (c) NS-pHC-0.674, (d) NS-pHC-1.348.

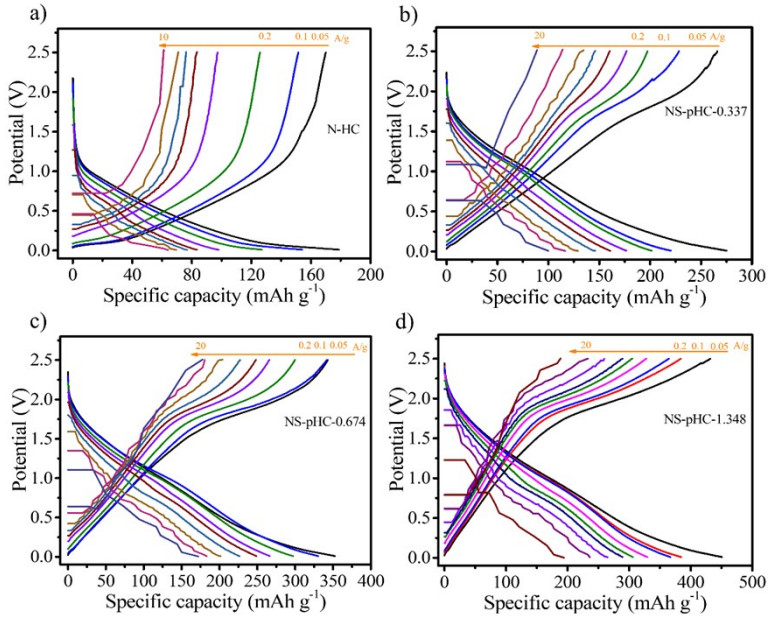


**Fig. S10.** The GCD curves at different current densities. (a) N-HC, (b) NS-pHC-0.337, (c) NS-pHC-0.674, (d) NS-pHC-1.348.

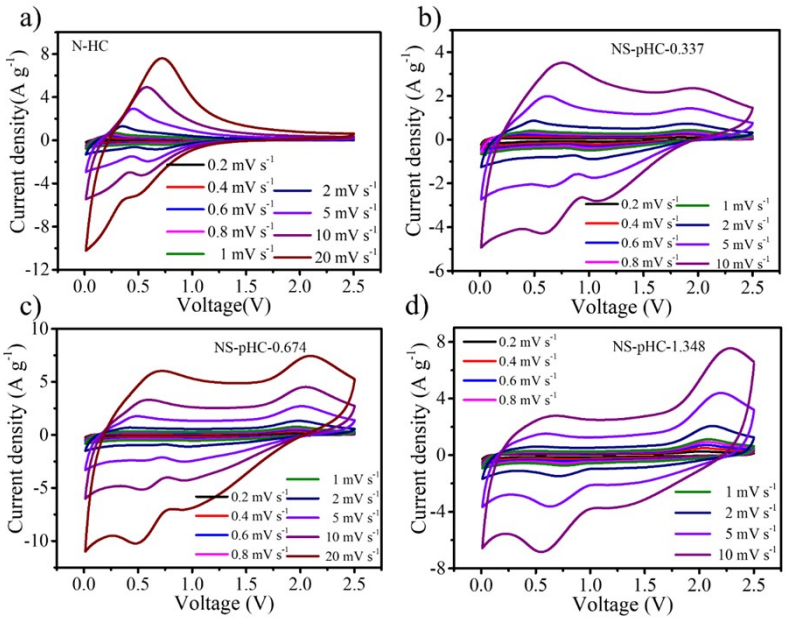


**Fig. S11.** The CV curves at different scan speeds. (a) N-HC, (b) NS-pHC-0.337, (c) NS-pHC-0.674, (d) NS-pHC-1.348.

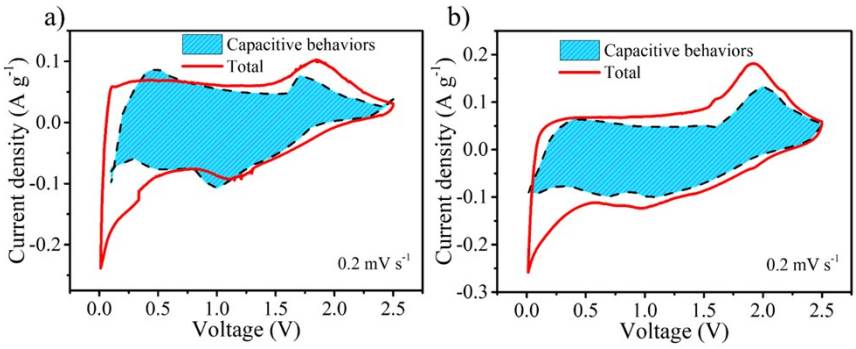


**Fig. S12.** The capacitive contribution (blue dashed area) of (a) NS-pHC-0.337 and (b) NS-pHC-0.674 at 0.2 mV $s^{-1}$.

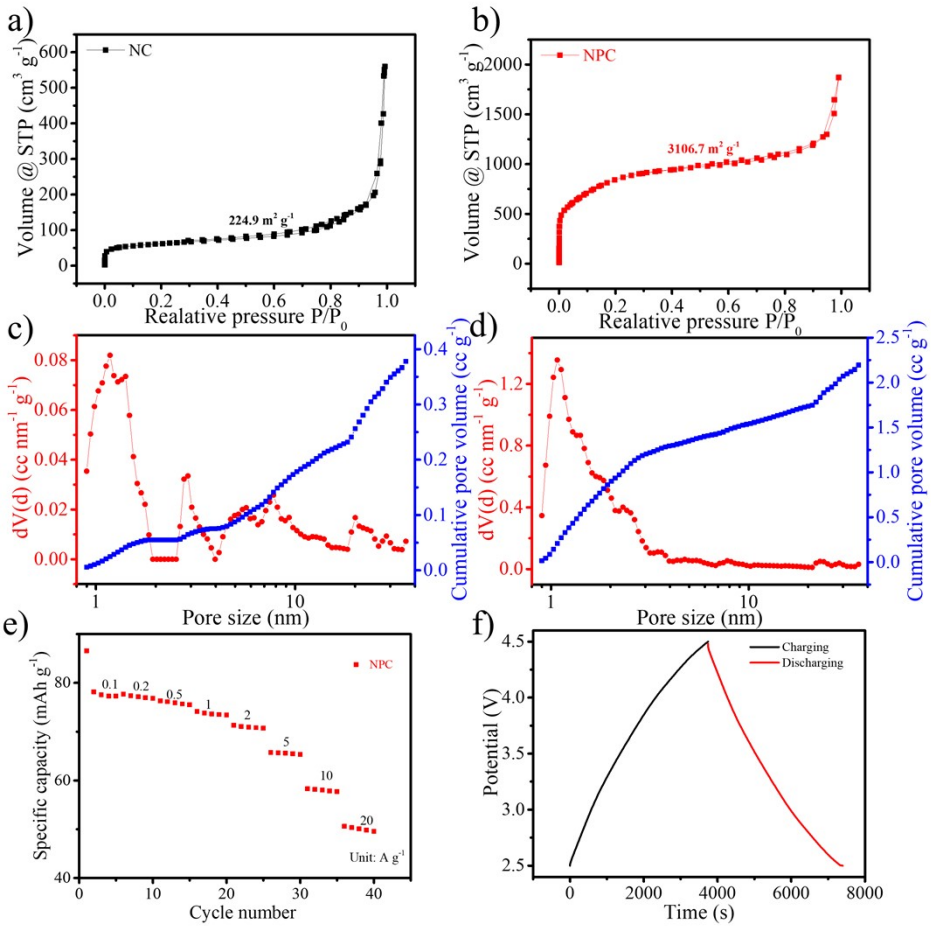


**Fig. S13.** The nitrogen adsorption/desorption curves of (a) NC and (b) NPC. The pore size distribution of (c) NC and (d) NPC. The rate performance (e) from 0.1 A $g^{-1}$ to 20 A $g^{-1}$ and GCD curve (f) at 0.1 A $g^{-1}$ of NPC.

**Table S1.** The structural parameters of N-HC and NS-pHC-*x* samples.

| Sample | 2 Theta $_{(002)}$ | SSA $m^2g^{-1}$ | Micropores size nm | Mesopores size nm | $I_D/I_G$ |
|---|---|---|---|---|---|
| N-HC | 24.9° | 41.2 | 1.7 | / | 2.44 |
| NS-pHC-0.337 | 25.3° | 88.1 | 1.40 | / | 2.46 |
| NS-pHC-0.674 | 25.3° | 566.2 | 1.07 | 2-4 | 2.75 |
| NS-pHC-1.348 | 25.5° | 854.5 | 1.07 | 2-4 | 2.97 |

**Table S2.** The surface chemical state parameters of N-HC and NS-pHC-*x* samples.

| Sample | Pyridinic N (at%) | Pyrrolic N (at%) | Quaternary N (at%) | C-S-C (at%) | Total N (at%) | Total S (at%) |
|---|---|---|---|---|---|---|
| N-HC | 4.68 | 4.42 | 1.95 | 0.39 | 12.07 | 0.78 |
| NS-pHC-0.337 | 5.04 | 4.66 | 1.08 | 3.45 | 11.54 | 4.36 |
| NS-pHC-0.674 | 4.98 | 4.35 | 0.87 | 5.52 | 11.02 | 6.11 |
| NS-pHC-1.348 | 5.41 | 4.20 | 0.72 | 7.12 | 11.31 | 7.77 |

**Table S3.** The comparison of ICE and rate performance of NS-pHC-1.348 with those reported in the literatures.

| Sample | ICE | Capacity mAh $g^{-1}$ (Current density A $g^{-1}$) | Reference |
|---|---|---|---|
| NS-pHC-1.348 | 49.99% | **383.9 (0.05); 183.2 (20)** | This work |
| N, S co-doped nanoporous carbon | 47.7% | 322 (0.2); 172 (10) | [1] *Energy Storage Mater* 2018, ***11***, 274-281. |
| N, S co-doped carbon microspheres | ≈80.8% | 210 (0.1); 131 at (5) | [2] *Adv Energy Mater* 2016, **6**, 1501929. |
| S, N co-doped mesoporous hollow carbon spheres | 29% | 240 (0.5); 138 (30) | [3] *Adv Energy Mater* 2019, ***9***, 1900036. |
| S-enriched N doped multichannel hollow carbon nanofiber | 62% | 329 (0.05); 132 (10) | [4] *Small* 2018, ***14***, e1802218. |
| S-doped N-rich carbon nanosheets | ≈43.9% | 350 (0.05); 110 (10) | [5] *Adv Mater* 2017, ***29***, 1604108. |
| N, S co-doped porous carbon nanosheets | 34.4% | 294.6 (0.1); 176 (2) | [6] *Chem Eng J* 2019, ***364***, 208-216. |
| N, S co-doped graphene nanosheets | 50.86% | 400 (0.03); 141 (5) | [7] *Energy Storage Mater* 2018, ***13***, 134-141. |

**Table S4.** The electrochemical property parameters of N-HC and NS-pHC-x.

| Sample | ICE | Capacity mAh $g^{-1}$ (Current density A $g^{-1}$) | Cycle (at 1 A $g^{-1}$) | Capacity proportion below 0.1 V at 3rd cycle at 0.05 A $g^{-1}$ | Capacitive behaviors proportion at 0.2 mV $s^{-1}$ |
|---|---|---|---|---|---|
| N-HC | 48.81% | 161.2 (0.05); 33.3 (20) | 81.3 (102%) | 52.9 (29.6%) | 49.82% |
| NS-pHC-0.337 | 60.65% | 241.3 (0.05); 88.9 (20) | 169.7 (84.8%) | 38.3 (13.9%) | 72.04% |
| NS-pHC-0.674 | 54.96% | 327.9 (0.05); 172.2 (20) | 199 (79.5%) | 46.2 (13.1%) | 68.59% |
| NS-pHC-1.348 | 49.99% | 383.9 (0.05); 183.2 (20) | 287.2 (87.0%) | 54.7 (11.7%) | 70.19% |

## REFERENCES


1 Y. Liu, Y. Qiao, G. Wei, S. Li, Z. Lu, X. Wang and X. Lou, Energy Storage Mater., 2018, **11**, 274-281.

2 D. F. Xu, C. J. Chen, J. Xie, B. Zhang, L. Miao, J. Cai, Y. H. Huang and L. N. Zhang, Adv. Energy Mater., 2016, **6**, 1501929.

3 D. Ni, W. Sun, Z. Wang, Y. Bai, H. Lei, X. Lai and K. Sun, Adv. Energy Mater., 2019, **9**, 1900036.

4 X. Sun, C. Wang, Y. Gong, L. Gu, Q. Chen and Y. Yu, Small, 2018, **14**, e1802218.

5 J. Yang, X. Zhou, D. Wu, X. Zhao and Z. Zhou, Adv. Mater., 2017, **29**, 1604108.

6 X. Miao, D. Sun, X. Zhou and Z. Lei, Chem. Eng. J., 2019, **364**, 208-216.

7 Y. Ma, Q. Guo, M. Yang, Y. Wang, T. Chen, Q. Chen, X. Zhu, Q. Xia, S. Li and H. Xia, Energy Storage Mater., 2018, **13**, 134-141.